2nd International Summer School on Nuclear Glass Wasteform: Structure, Properties and Long-Term Behavior, SumGLASS 2013

Simulations of phase-field models for crystal growth and phase separation

Alain Cartalade[a,*], Amina Younsi[a], Élise Régnier[b], Sophie Schuller[b]

[a]CEA–Saclay, DEN, DM2S, STMF, LATF, Gif-sur-Yvette F-91191, France
[b]CEA–Marcoule, DEN, DTCD, SECM, LDMC, Bagnols-sur-Cèze F-30207, France

Abstract

Phase-field theory is a thermodynamically consistent approach for modeling and simulating phenomena that exhibit complex structures such as those encountered in fluid flows and materials science. In this work, the main features of the theory will be reviewed, i.e. mathematical models which arise from the minimization of a thermodynamic potential such as the Helmholtz free energy describing the phenomenology of bulk phases and their interactions. An order parameter is also introduced which plays the role of a phase index avoiding to track explicitly the interface between liquid/liquid and liquid/solid phases. Next, various examples will be given on the basis of phenomena observed in nuclear glasses. Simulations are divided into two classes: for a non-conserved order parameter, simulations will be presented on crystal growth of a pure substance with and without hydrodynamic effect. For a conserved order parameter, an example will be given on phase separation by spinodal decomposition. Finally, the discussion will focus on the parameters needed for the phase-field models and their relationships with the sharp interface approach.

1. Introduction

In the vitrification process of radioactive waste with the cold crucible technique (Lemonnier et al., 2012), the gradient of temperature imposed to the system (Sauvage et al., 2010), associated with a complex composition of glass, leads at local scale to several phenomena involving interfaces. In this work, we focus on the simulation of two chemico-physical phenomena observed in glasses: the crystal growth and the spinodal decomposition. The first one is liquid/solid phase transition, where interface is located between a liquid phase and a solid phase. A good review about instabilities and pattern formation in crystal growth can be found in Langer (1980). The second one is fluid mechanics involving two immiscible liquids which spontaneously separate. An illustration of crystal growth is given by a borosilicate glass heated between 600°C and 900°C. This range of temperature is favorable for observing crystals of calcium molybdate and apatites with the scanning electron microscopy (Delattre et al., 2013). The solidification process can be summarized as follows: when the temperature is lowered below the melting temperature, nuclei are

---

* Corresponding author. Tel.: +33(0)-169-084-067 ; fax: +33(0)-169-088-229.
E-mail address: alain.cartalade@cea.fr (Alain Cartalade).

likely to appear and grow, releasing latent heat at the solid/glass interface. First, the growing speed of crystal increases when the temperature is decreased. Then, as the glass becomes more and more viscous, the speed decreases (Scholze, 1980). The second example is the phase separation phenomenon. Depending on the temperature and composition of glass system, a spinodal regime or a nucleation and growth regime can be observed (Hodroj et al., 2013). Typically, when the phase separation mechanism occurs by nucleation and growth, disconnected and spherical (or globular) phases are dispersed in a residual matrix, separated by a sharp interface (Schuller et al., 2011). Conversely, phase separation by spinodal decomposition, results in strongly interconnected phases (Bouttes et al., 2013) separated by diffuse interfaces with varying compositions over time.

Concerning crystal growth and phase separation, modeling of both can be thought in a same theoretical framework. Simulations require calculating the interface position in space and time as well as temperature or/and fluid velocity. In order to follow the interface position, several modeling methods exist in the literature, mainly divided into two classes: the separation between each phase can be considered as a sharp interface or a diffuse one. In this work, we present an introduction of phase-field theory, a diffuse interface method that is consistent with the thermodynamics of the system. Several topical reviews exist on phase-field models for materials science (Boettinger et al., 2002; Singer-Loginova and Singer, 2008; Provatas and Elder, 2010) and fluid mechanics (Anderson et al., 1998). In this paper, we focus on the main features of the theory (section 2) that will be illustrated on the simulation of one particular problem from each domain (section 3). For crystal growth, simulations will present sensitivity of undercooling and hydrodynamic effect on the crystal shape. For phase separation, one simulation will be carried out on spinodal decomposition. Finally, the section 4 will be dedicated to a discussion about difficulties of applying phase-field models in complex systems such as glasses.

2. Phase-field theory

2.1. Order parameter, free energy and equations of motion

One of the main feature of the phase-field theory is the introduction of a new function, the phase-field $\phi(\mathbf{x}, t) \equiv \phi$ depending on position $\mathbf{x}$ and time t. The phase-field is also called index function or order parameter. This function describes the bulk phases and the diffuse interface separating them. For instance, in solidification problems, $\phi = +1$ describes the solid phase and $\phi = -1$ describes the liquid phase. Between both values, the phase-field is continuous and varies smoothly: $-1 < \phi < +1$. The interface position between both phases is described by the variation of ϕ in space.

The second most important feature of the theory is relative to the model derivation which is thermodynamically consistent. In such models, partial derivative equations derive from a free energy (or entropy) functional $\mathcal{F}$ which must be minimized (resp. maximized). The free energy functional describes the bulk phases and their interaction. The gradient of order parameter $\boldsymbol{\nabla}\phi$ explicitly appears in its definition. Thermodynamic relationships are next used in the variational procedure as well as the conservation equations (e.g., Wang et al., 1993).

In solidification problem, the order parameter is not a conserved quantity and obeys to the dynamics of Allen-Cahn equation also called model A (see classification in Hohenberg and Halperin, 1977). For phase separation, the order parameter is related to the conserved quantities such as the number of molecules (see subsection 2.3). In that case, ϕ follows the dynamics of Cahn-Hilliard equation (model B). Two specific examples of free energy functional and equations of motion for ϕ are given below. For sake of simplicity, all parameters are assumed to be constant and equal in each phase. In crystal growth simulations, only a pure substance is considered.

2.2. Crystal growth of a pure substance: Karma and Rappel model

For the solidification process of binary mixtures, phase-field models can be found in Echebarria et al. (2004) for directional solidification, and Ramirez et al. (2004) and Kim et al. (1999) for binary solidification coupled with temperature. However, in this section, we assume for simplicity the solidification process of a pure (or congruent)

substance, and we assume that the specific heat C_p and thermal diffusivity κ are identical in each phase. In this case, the free energy functional writes:

$$\mathcal{F}_{KR} = \int_V \left[\frac{W^2(\mathbf{n})}{2} |\boldsymbol{\nabla}\phi|^2 + f_{dw}(\phi) + \lambda u g(\phi) \right] dV, \tag{1}$$

where $W(\mathbf{n})$ is the interface width depending on the normal vector of interface $\mathbf{n} = -\boldsymbol{\nabla}\phi/|\boldsymbol{\nabla}\phi|$, pointing from solid to liquid. The function $f_{dw}(\phi)$ is the standard double-well potential, $f_{dw}(\phi) = -\phi^2/2 + \phi^4/4$, defined in this model such as the two minima are $\phi = +1$ and $\phi = -1$. The coupling with the temperature is given by the last term $\lambda u g(\phi)$, where λ is the coupling coefficient and $u \equiv u(\mathbf{x}, t)$ is the dimensionless temperature defined as: $u(\mathbf{x}, t) = C_p(T(\mathbf{x}, t) - T_m)/L$. The latent heat is noted L and T_m is the melting temperature. $g(\phi) = (15/8)(\phi - 2\phi^3/3 + \phi^5/5)$ is a monotonous interpolation function of internal energy inside the diffuse zone. The specific form of the coupling term is obtained by performing the difference between the free energy densities of solid and liquid. This term represents the driving force of the solidification process. The phase-field model is derived from Eq. (1) by calculating the time derivative. The phase-field equation and heat equation are respectively given by (Karma and Rappel, 1998):

$$\tau(\mathbf{n})\frac{\partial\phi}{\partial t} = W_0^2 \boldsymbol{\nabla} \cdot (a_s^2(\mathbf{n})\boldsymbol{\nabla}\phi) + W_0^2 \sum_{\alpha=x,y,z} \frac{\partial}{\partial\alpha}\left(|\boldsymbol{\nabla}\phi|^2 a_s(\mathbf{n})\frac{\partial a_s(\mathbf{n})}{\partial(\partial_\alpha\phi)}\right) + (\phi - \phi^3) - \lambda u(1 - \phi^2)^2, \tag{2a}$$

$$\frac{\partial u}{\partial t} = \kappa \boldsymbol{\nabla}^2 u + \frac{1}{2}\frac{\partial\phi}{\partial t}. \tag{2b}$$

Eq. (2a) is the equation of motion of interface. The first term of the right-hand side is a diffusive term, the second one is responsible of anisotropic growth where $\partial_\alpha \equiv \partial/\partial\alpha$ with $\alpha = x, y, z$, the third one is the derivative of the double-well potential with respect to ϕ. The last one is the derivative with respect to ϕ of the coupling term with the temperature. Eq. (2b) is the standard equation of diffusion for dimensionless temperature with an additional source term $(1/2)\partial_t\phi$. The physical meaning of this term is the release of latent heat at interface. Anisotropy in the surface energy and in the kinetics is incorporated as in Kobayashi (1993) and Wheeler et al. (1993) via the dependence of $W(\mathbf{n})$ and $\tau(\mathbf{n})$. This dependence is taken into account by a unique anisotropy function $a_s(\mathbf{n})$ with $\tau(\mathbf{n}) = \tau_0 a_s(\mathbf{n})$ and $W(\mathbf{n}) = W_0 a_s(\mathbf{n})$ where τ_0 and W_0 are two constants. The function $a_s(\mathbf{n})$ is defined as:

$$a_s(\mathbf{n}) = 1 - 3\varepsilon_s + 4\varepsilon_s \frac{(\partial_x\phi)^4 + (\partial_y\phi)^4 + (\partial_z\phi)^4}{|\boldsymbol{\nabla}\phi|^4}, \tag{2c}$$

where ε_s is the strength of anisotropy.

2.3. Spinodal decomposition: Navier-Stokes/Cahn-Hilliard model

In this second example, the order parameter describes the composition of two immiscible fluids A and B (binary mixture). To be consistent with the previous subsection, the composition is defined as: $\phi = (n_A - n_B)/(n_A + n_B)$ where n_A and n_B are the number of molecules of A and B respectively. With this definition, the A-fluid is locally indicated by $\phi = +1$ (for $n_B = 0$) and the B-fluid is indicated by $\phi = -1$ (for $n_A = 0$). A mixture of both fluids A and B is characterized by $-1 < \phi < +1$. The order parameter is now a conserved quantity. The equation of motion is derived from the free energy functional defined as (Cahn and Hilliard, 1958):

$$\mathcal{F}_{CH} = \int_V \left[\frac{\sigma}{2} |\boldsymbol{\nabla}\phi|^2 + H f_{dw}(\phi) \right] dV, \tag{3}$$

where σ is the coefficient of gradient energy and H is the height of double-well potential. The Cahn-Hilliard (CH) equation with an advective term writes (Jasnow and Viñals, 1996; Jacqmin, 1999):

$$\frac{\partial\phi}{\partial t} = \boldsymbol{\nabla} \cdot (M_\phi \boldsymbol{\nabla}\mu_\phi - \mathbf{V}\phi), \tag{4a}$$

which involves two fluxes: the first one is given by the product of the interfacial mobility $M_\phi > 0$, times the opposite gradient of chemical potential $-\nabla\mu_\phi$. The second one is the advective flux $\mathbf{V}\phi$ where $\mathbf{V}$ is the velocity. The chemical potential measures the change of free energy for a small local change of composition: $\mu_\phi = \delta\mathcal{F}/\delta\phi$. By using the definition of CH free energy (Eq. (3)), the chemical potential is:

$$\mu_\phi = H(\phi^3 - \phi) - \sigma\nabla^2\phi. \tag{4b}$$

The velocity $\mathbf{V}$ is given by the Navier-Stokes (NS) equations:

$$\nabla \cdot \mathbf{V} = 0, \tag{4c}$$

$$\rho\left[\frac{\partial\mathbf{V}}{\partial t} + (\mathbf{V}\cdot\nabla)\mathbf{V}\right] = -\nabla p + \eta\nabla^2\mathbf{V} - \phi\nabla\mu_\phi, \tag{4d}$$

where $\rho = (n_A + n_B)/2$ is the mean density of mixture, η is the dynamical viscosity and p is the pressure. Eq. (4c) is the mass conservation equation for an incompressible fluid. The second one expresses the momentum conservation with a body force (last term in the right-hand side) for modeling the capillary effects in the diffuse-interface framework.

3. Simulations

Eqs. (2a)–(2c) for crystal growth and Eqs. (4a)–(4d) for spinodal decomposition are simulated by using a numerical method based on the Lattice Boltzmann (LB) equation (Chen and Doolen, 1998; Guo and Shu, 2013). For spinodal decomposition, the LB method has already been applied in several works (e.g. Kendon et al., 2001). In this paper, the numerical method is inspired from Zheng et al. (2006). For crystal growth problems, the LB method was applied for hydrodynamic equations in Medvedev and Kassner (2005) and Chatterjee and Chakraborty (2006). For Karma-Rappel model, numerical implementations of LB method are detailed in Cartalade (2013) and Younsi (2013).

3.1. Crystal growth of a pure substance

Undercooling sensitivity. The undercooling is defined as the initial temperature $T_0 \equiv T(\mathbf{x}, 0)$ taken below the melting temperature T_m: $u_0 = C_p(T_0 - T_m)/L < 0$, which is equivalent to a negative dimensionless temperature u_0. When the deviation of temperature is important between T_0 and T_m, the latent heat released at interface during the solidification process can be evacuated more quickly into the liquid. A faster growth of crystal is experimentally observed (Scholze, 1980). For all simulations, the mesh is composed of 301^3 nodes. The initial condition is set as a nucleus of radius $R_s = 8$ lattice unit in the center of computational domain. All boundary conditions are zero fluxes for phase-field and temperature equations. Parameters are $\lambda = 10$, $\kappa = 0.7$, $\tau_0 = 10^{-4}$ and $W_0 = 10^{-2}$. The parameter ε_s is responsible of the crystal shape: if this parameter is zero, the function $a_s(\mathbf{n})$ (Eq. (2c)) is a constant and the second term of the right-hand side of Eq. (2a) cancels. The evolution of that case leads to a spherical shape. In the following simulations, we choose $\varepsilon_s = 0.05$. The time-step is $\delta t = 1.5 \times 10^{-5}$ and the space step is $\delta x = 10^{-2}$. Crystal shapes (iso-values $\phi = 0$) are compared in Fig. 1 for $u_0 = -0.2$ (Fig. 1a), $u_0 = -0.25$ (Fig. 1b) and $u_0 = -0.3$ (Fig. 1c). As expected, we remark that a larger value of undercooling (resp. a lower value of initial temperature u_0) involves a crystal growth that is faster. Notice that for a binary mixture, the crystal growth is also influenced by the solute diffusion mechanisms. In that case, the competition between the heat and mass transfer is quantified by the Lewis number defined as the ratio between the thermal diffusivity and the diffusion coefficient (Younsi et al., 2014).

Hydrodynamic effect on crystal shape. The crystal growth is also influenced by the fluid flows of the liquid phase. In order to study the hydrodynamics effect on crystal growth, Eqs. (2a)–(2b) have to be coupled with the Navier-Stokes equations. The hydrodynamic model and the specific form of coupling terms are inspired from Beckermann et al. (1999). In this model, the phase-field equation is unchanged, an advective term is added in the heat equation and a force term is also added in the momentum equation. The phase-field ϕ is not used directly in the heat equation and Navier-Stokes equations: the advective terms inside the solid part are canceled by using a new function $\psi = (1 - \phi)/2$ which is equal to 0 in the solid and +1 in the liquid. For simulations, the values of parameters are identical as those
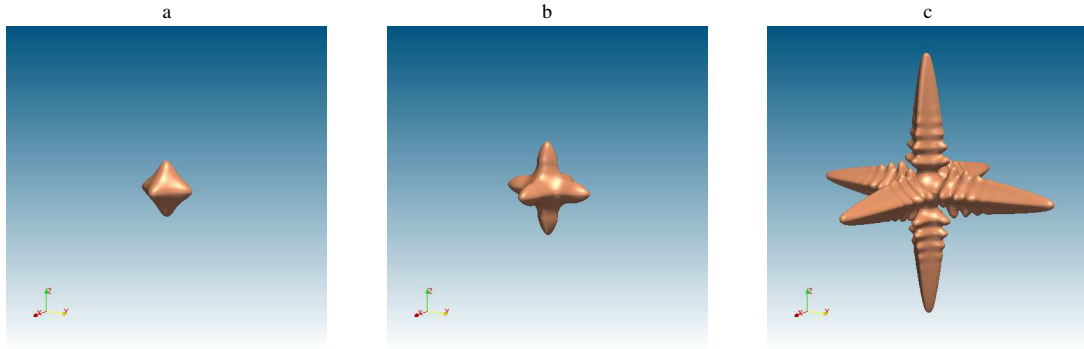
Figure 1. Undercooling effect on crystal shape. Iso-values $\phi = 0$ at $t = 5000\delta t$ for (a) $u_0 = -0.20$, (b) $u_0 = -0.25$ and (c) $u_0 = -0.30$.
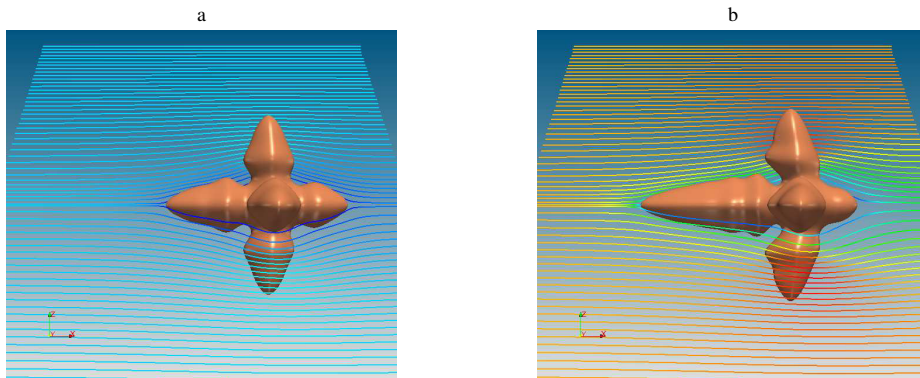

Figure 2. Hydrodynamic effect on crystal growth for a flow directed from left to right (a) Initial velocity V_1; (b) Initial velocity $V_2 = 4V_1$.

used for undercooling sensitivity. An initial velocity is applied directed from left to right. Results are presented in Fig. 2 for two values of initial velocity V_1 and V_2 with $V_2 = 4V_1 > V_1$. We remark that the crystal is not any more symmetric: one side of the crystal grows faster than the other ones, and the growth is faster with a greater initial velocity. Results are consistent with those presented in Chen et al. (2009). The explanation is given by temperature gradients that are higher upstream rather than downstream. The latent heat can be evacuated more quickly upstream and the side branch can grow faster.

3.2. Spinodal decomposition

In glasses, hydrodynamic parameters such as viscosity and density are very dependent on temperature (Jacoutot, 2006). In this work, the spinodal decomposition is illustrated for a fixed temperature in the glass melt and hydrodynamic parameters that are constant. Boundary conditions are periodic for all faces. The mesh is composed of 251^3 nodes, $\delta t = 3 \times 10^{-3}$ and $\delta x = 0.01$. As initial condition, the order parameter is randomly distributed between -1 and $+1$ in whole domain and the initial velocity is zero. Parameters relative to CH equation are $\sigma = 3 \times 10^{-7}$ and $H = 0.01$ corresponding to an interface width equal to $W = 2 \times 10^{-2}$, the kinematic viscosity is $\nu = 5 \times 10^{-3}$ and the density is $\rho = 3$. The time evolution of phase-field ϕ is illustrated in Fig. 3. The initial mixture is homogeneous (Fig. 3a) and spontaneously separates into two phases by minimizing the free energy of the system. After an early period of interdiffusion (Fig. 3b and 3c), two main regions appear (Fig. 3d). The A-fluid (red) and the B-fluid (blue) are separated by a diffuse interface (green) where both phases coexist. Finally, each phase can grows by coalescence (Fig. 3e–h).
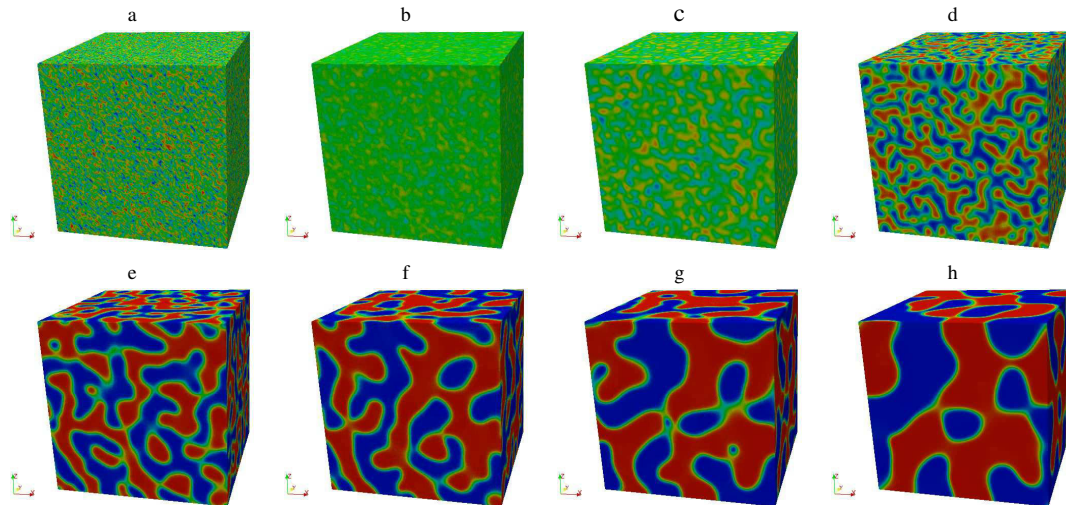
Figure 3. Phase separation by spinodal decomposition of two immiscible liquids *A* ($\phi = +1$; red) and *B* ($\phi = -1$; blue).

4. Conclusion

Phase-field models are powerful tools for simulating physical problems involving interfaces. They introduce an order parameter defined over the whole computational domain and they are consistent with the thermodynamic of the system. For instance, models can be solved effectively in 3D, without tracking the interfacial surface between phases, in order to simulate the spinodal decomposition and the crystal growth with or without hydrodynamics. Nevertheless some theoretical issues still remain to be solved in phase-field models (Plapp, 2011). Moreover, they require a lot of experimental data and some of them are difficult to measure, in particular the interfacial energy between glass and crystals (Fokin et al., 2000). Notice that in the case of pure substances, these quantities may be derived from molecular dynamic simulations (Bragard et al., 2002; Nestler et al., 2005).

For glasses that are multi-species systems, a further problem arises. In phase-field approach, the interfacial boundary conditions such as the energy balance equation and the temperature correction, are replaced by the phase-field equation. The connection between this approach with the sharp interface model is carried out by performing a mathematical analysis called "matched asymptotic expansions". This analysis yields relationships between the parameters of the phase-field equation ($W(\mathbf{n})$, $\tau(\mathbf{n})$, and λ) and the physical parameters such as the capillary length and the kinetic coefficient (Karma and Rappel, 1998; Almgren, 1999). For a binary mixture with different values of diffusion in solid and liquid, this analysis leads to a phenomenological anti-trapping current that has to be added in the supersaturation equation (Karma, 2001). This mathematical procedure was applied for binary mixtures in solidification problems (Ohno, 2012) and fluid mechanics (Sibley et al., 2013), but still remains to be done for multi-species systems.

Acknowledgements

References

Almgren, R.F., 1999. Second-order phase field asymptotics for unequal conductivities. Siam Journal on Applied Mathematics 59, 2086–2107.
Anderson, D., McFadden, G., Wheeler, A., 1998. Diffuse-interface methods in fluid mechanics. Annual Reviews of Fluid Mechanics 30, 139–165.
Beckermann, C., Diepers, H.J., Steinbach, I., Karma, A., Tong, X., 1999. Modeling melt convection in phase-field simulations of solidification. Journal of Computational Physics 154, 468–496.
Boettinger, W.J., Warren, J.A., Beckermann, C., Karma, A., 2002. Phase-field simulation of solidification. Annual Review of Materials Research 32, 163–194.

Bouttes, D., Gouillart, E., Dalmas, D., Vandembroucq, D., 2013. In situ observation of coarsening in a phase-deparated glass. AIP Conference Proceedings 1518, 487.

Bragard, J., Karma, A., Lee, Y.H., Plapp, M., 2002. Linking phase-field and atomistic simulations to model dendritic solidification in highly undercooled melts. Interface Science 10, 121–136.

Cahn, J., Hilliard, J., 1958. Free energy of a nonuniform system. i. interfacial free energy. Journal of Chemical Physics 28, 258–267.

Cartalade, A., 2013. Simulations par méthode de Boltzmann sur réseau d'un modèle à champ de phase pour les problèmes de croissance cristalline II : Modèle avec limite à interface fine d'une substance pure 3D. Technical Report NT/13-008/A. CEA–Saclay, DEN, DM2S, STMF, LATF.

Chatterjee, D., Chakraborty, S., 2006. A hybrid lattice boltzmann model for solid-liquid phase transition in presence of fluid flow. Physics Letters A 351, 359–367.

Chen, C.C., Tsai, Y.L., Lan, C.W., 2009. Adaptive phase field simulation of dendritic crystal growth in a forced flow: 2d vs 3d morphologies. International Journal of Heat and Mass Transfer 52, 1158–1166.

Chen, S., Doolen, G., 1998. Lattice boltzmann method for fluid flows. Annual Reviews of Fluid Mechanics 30, 329–364.

Delattre, O., Régnier, E., Schuller, S., Allix, M., Matzen, G., 2013. Image analysis study of crystallization in two glass compositions of nuclear interest. Journal of Non-Crystalline Solids 379, 112–122.

Echebarria, B., Folch, R., Karma, A., Plapp, M., 2004. Quantitative phase-field model of alloy solidification. Physical Review E 70, 1–22.

Fokin, V., Zanotto, E., Schmelzer, J., 2000. Method to estimate crystal/liquid surface energy by dissolution of subcritical nuclei. Journal of Non 278, 24–34.

Guo, Z., Shu, C., 2013. Lattice Boltzmann Method and its Applications in Engineering. volume 3 of *Advances in Computational Fluid Dynamics*. World Scientific Publishing Co. Pte. Ltd.

Hodroj, A., Simon, P., Florian, P., Chopinet, M.H., Vaills, Y., 2013. Phase separation and spatial morphology in sodium silicate glassesby afm, light scattering and nmr. J. Am. Ceram. Soc. 96, 2454?–2460.

Hohenberg, P.C., Halperin, B.I., 1977. Theory of dynamic critical phenomena. Reviews of Modern Physics 49, 435–479.

Jacoutot, L., 2006. Modélisation numérique de phénomènes couplés dans des bains de verre brassés mécaniquement et élaborés en creuset froid inductif. Ph.D. thesis. INPG.

Jacqmin, D., 1999. Calculation of two-phase navier-stokes flows using phase-field modeling. Journal of Computational Physics 155, 96–127.

Jasnow, D., Viñals, J., 1996. Coarse-grained description of thermo-capillary flow. Physics of Fluids 8, 660–669.

Karma, A., 2001. Phase-field formulation for quantitative modeling of alloy solidification. Physical Review Letters 87, 1–4.

Karma, A., Rappel, W.J., 1998. Quantitative phase-field modeling of dendritic growth in two and three dimensions. Physical Review E 57, 4323–4349.

Kendon, V., Cates, M., Pagonabarraga, I., Desplat, J.C., Bladon, P., 2001. Inertial effects in three-dimensional spinodal decomposition of a symmetric binary fluid mixture: a lattice boltzmann study. Journal of Fluid Mechanics 440, 147–203.

Kim, S.G., Kim, W.T., Suzuki, T., 1999. Phase-field model for binary alloys. Physical Review E 60, 7186–7197.

Kobayashi, R., 1993. Modeling and numerical simulations of dendritic crystal growth. Physica D 63, 410–423.

Langer, J.S., 1980. Instabilities and pattern formation in crystal growth. Reviews of Modern Physics 52, 1–28.

Lemonnier, S., Labe, V., Ledoux, A., Nonnet, H., Godon, N., Naline, S., 2012. Methodology of qualification of ccim vitrification process applied to the high-level liquid waste from reprocessed oxide fuels, in: Waste Management Symposia (WM2012), February 26-March 1, Phoenix, AZ.

Medvedev, D., Kassner, K., 2005. Lattice boltzmann scheme for crystal growth in external flows. Physical Review E 72, 1–10.

Nestler, B., Danilov, D., Galenko, P., 2005. Crystal growth of pure substances: Phase-field simulations in comparison with analytical and experimental results. Journal of Computational Physics 207, 221–239.

Ohno, M., 2012. Quantitative phase-field modeling of nonisothermal solidification in dilute multicomponent alloys with arbitrary diffusivities. Physical Review E 86, 1–15.

Plapp, M., 2011. Remarks on some open problems in phase-field modelling of solidification. Philosophical Magazine 91, 25–44.

Provatas, N., Elder, K., 2010. Phase-Field Methods in Materials Science and Engineering. Wiley-VCH.

Ramirez, J.C., Beckermann, C., Karma, A., Diepers, H.J., 2004. Phase-field modeling of binary alloy solidification with coupled heat and solute diffusion. Physical Review E 69, 1–16.

Sauvage, E., Brun, P., Bonnetier, A., Lacombe, J., Chauvin, E., 2010. 3-d thermal, hydrodynamic & magnetic modelling of elaboration of glass by induction in cold crucible, in: Waste Management Symposia (WM2010), March 7-11, Phoenix, AZ.

Scholze, H., 1980. Glass – nature, structure and properties. Springer.

Schuller, S., Pinet, O., Penelon, B., 2011. Liquid-liquid phase separation process in borosilicate liquids enriched in molybdenum and phosphorus oxides. Journal of the American Ceramic Society 94, 447–454.

Sibley, D., Nold, A., Kalliadasis, S., 2013. Unifying binary fluid diffuse-interface models in the sharp-interface limit. Journal of Fluid Mechanics 736, 5–43.

Singer-Loginova, I., Singer, H.M., 2008. The phase field technique for modeling multiphase materials. Reports on Progress in Physics 71, 1–32.

Wang, S.L., Sekerda, R.F., Wheeler, A.A., Murray, B.T., Coriell, S.R., Braun, R.J., McFadden, G.B., 1993. Thermodynamically-consistent phase-field models for solidification. Physica D 69, 189–200.

Wheeler, A.A., Murray, B.T., Schaefer, R.J., 1993. Computation of dendrites using phase field model. Physica D 66, 243–262.

Younsi, A., 2013. Simulations par méthode de Boltzmann sur réseau d'un modèle à champ de phase pour les problèmes de croissance cristalline III : solidification d'un mélange binaire dilué. Technical Report NT/13-033/A. CEA–Saclay, DEN, DM2S, STMF, LATF.

Younsi, A., Cartalade, A., Quintard, M., 2014. Lattice boltzmann simulations for anisotropic crystal growth of a binary mixture, in: Proceedings of the 15th International Heat Transfer Conference, IHTC15, August 10–15, Kyoto, Japan. (Accepted – To be published).

Zheng, H., Shu, C., Chew, Y., 2006. A lattice boltzmann model for multiphase flows with large density ratio. Journal of Computational Physics 218, 353–371.